

Lens design based on instantaneous focal function

Sung Nae Cho*

*MEMS & Packaging Group, Micro Systems Lab, Samsung Advanced Institute of Technology,
Mt. 14-1 Nongseo-dong Giheung-gu, Yongin-si Gyeonggi-do, 446-712, South Korea.*

(Dated: Prepared on January 30, 2009)

The formula for the lens is derived based on the information of instantaneous focal function. Focal function is an important tool in designing lenses with extended depth of focus (EDoF) because this allows **EDoF** lens designers to try out various mathematical curves using computers to optimize their design. Once an optimal focal function information is obtained, the corresponding physical **EDoF** lens can be fabricated using the lens equation formulated in this presentation.

I. INTRODUCTION

Optical imaging system with large depth of field (**DOF**) is required to produce sharp images(**author?**) [1]. In photography, the **DOF** is the portion of a scene that appears sharp in the image, for example, the region denoted by **A** in Fig. 1. Ordinarily, a lens focuses parallel rays of light at one distance known as the focal point, as illustrated in Fig. 2. Therefore, not all points within the **DOF** can be claimed as focused per se. However, due to a gradual decrease in the sharpness of the image from the focused spot, the amount of blurring within the **DOF** is imperceptible to human eyes under normal viewing conditions. As such, in particularly for films and photography, the image region can be subdivided into two, where one lies within and the other lies external to the **DOF**. In the photograph of Fig. 1, the region **A**, wherein the image appears sharp and focused, is said to lie within the **DOF**; whereas the region **B**, in which region the image is blurred, is said to lie external to the **DOF**.

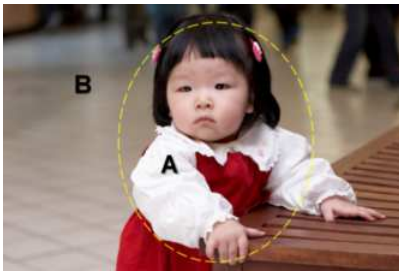


Figure 1: Illustration of depth of field. Region **A** is within the depth of field (**DOF**), whereas the region **B** is outside of **DOF**. The image is blurred drastically in region **B**.

Alternatively, but equivalently, the **DOF** in an imaging system is defined as the distance in the object space in which objects are considered to be in focus. The distance over which objects appear sharp can be increased by extending the **DOF** of an imaging system. Traditionally, the **DOF** of an imaging system can be increased

by either decreasing the size of lens aperture or by increasing the shutter speed, or through tweaking of the both. These methods, however, drastically reduces the amount of light passing through the lens and require extra lighting. For developing still images, the required extra lighting can be accommodated by the use of a flash. For motion pictures, however, this approach proves to be inadequate, as typical video involves about thirty frames of images per second.[15] In addition to this difficulty, the smaller lens aperture increases diffraction and this places a practical limit on the extent to which the **DOF** of an optical imaging system can be enhanced by the aforementioned methods. That being said, can the **DOF** of an imaging system be increased (**A**) without sacrificing the intensity of light passing through the lens and (**B**) without increasing the diffraction? The answer to this question is yes and this approach involves some sort of digital filtering.

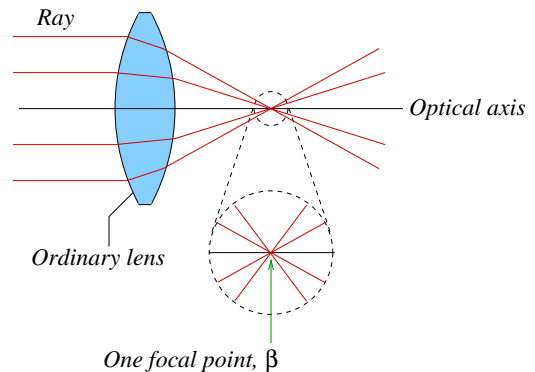


Figure 2: An ideal ordinary lens is characterized by a single focal point.

The digital filtering method requires a scheme for the image reconstruction algorithm based on the principles of wave optics(**author?**) [2, 3, 4, 5, 6, 7]. The image reconstruction code is often hardcoded in the accompanying digital processing unit (**DPU**) and, for this reason, the imaging method based on digital filtering is coined as the software assisted imaging technology or **SAIT** for short.[16] The **SAIT** solution for an imaging system is a promising technology in that it has potential to increase the **DOF** while encompassing altogether the processes of

*Electronic address: sungnae.cho@samsung.com

which (A) drastically reduce the amount of light passing through the lens and (B) those problems associated with increased diffraction due to the reduced diameter of the lens aperture.

The software assisted imaging technology is not as perfect as it sounds and it has some of its own problems to offer. Among them, one directly relates to the image processing speed. In the traditional imaging solutions based on lenses, which I refer to as the analog technology, complex arrangement of lenses function to focus image at the focal plane from wherein the image is developed. As such systems based on analog technology by-pass the digital filtering stage altogether, images are developed instantaneously in analog imaging systems. However, due to the aforementioned problems and limitations of the traditional method for increasing the **DOF**, the analog technology provides only a limited solution when concerning the image quality. The systems based on **SAIT** principle face problems that are exactly the opposite in nature from that of the analog systems. In principle, the reconstructed image by a way of image reconstruction algorithm can be made to resemble the original image to any level or degree of resemblance, provided the image processing speed is of no concern. But, such methodology would limit systems based on **SAIT** to still imagery applications and the video sector of the market must be discarded, which is a bad idea for business. Naturally, for systems based on **SAIT** principle, a trade off must be made between the image quality and the image processing speed.

Among the early pioneers to successfully commercialize imaging system based on **SAIT** are Cathay and Dowski, who did much of their work at the University of Colorado(**author?**) [5, 6, 7]. In the modern literature, their work is cited as “wavefront coding.” The **SAIT** solution based on wavefront coding has been trade marked by CDM Optics, Inc., and it is known as the Wavefront CodingTM. The imaging solution based on wavefront coding basically involves two stages: the input and the output stages. The input stage involves the optical element and this represents the hardware contribution side of the **SAIT** solution. The output stage involves the **DPU**, wherein the image reconstruction code base is hardcoded, and this represents the software contribution side of the **SAIT** solution. The optical element in **SAIT** solution is distinguished from the input stage of traditional imaging system, which is just complex series of ordinary lenses, in that it produces many focal points along the optical axis instead of just one at the focal plane. Such optical element is referred to as lens having extended depth of focus (or **EDoF** for short) and this is illustrated in Fig. 3.

Both the quality of reconstructed image and the image reconstruction speed are critically important in **SAIT**. In principle, the ordinary lens, such as the one illustrated in Fig. 2, can just as well serve as the input stage for the **SAIT** imaging systems. However, this must be done at the cost of overly complicated algorithm routines for the

software side of the system. The length of image reconstruction code directly relates to the number of transistors in a **DPU**. As a simple rule of a thumb, more transistors there are in a **DPU**, more energy it requires to operate. And, more lines of coding for the image reconstruction algorithm implies the slower processing speed for the reconstructed image output. The full-**HD** quality of a video involves sixty image frames every second. This implies, the application of **SAIT** system to full-**HD** video processing would require the image reconstruction time span of 16 ms or less. The demand for very fast processing speed and low power consumption make ordinary lenses inadequate for the input stage of the **SAIT** system, which leave open for an alternate solution for the optical element to be used as the input stage.

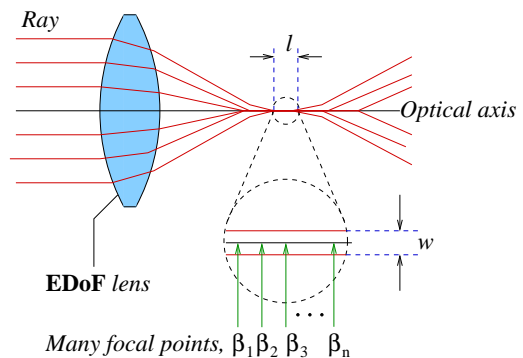


Figure 3: Lens with extended depth of focus has many focal points, f_1, f_2, f_3 , and so on. An ideal **EDoF** lens has infinitely many focal points and all light rays are confined within the cylindrical tube very small diameter w and very long length l .

The image reconstruction code base can be optimized for image processing speed and quality if the **EDoF** lens is used as the optical element for the input stage of **SAIT** system. The **EDoF** lens is characterized by parameters l and w . The parameter l represents the depth of focal points along the optical axis and the parameter w represents the width of bundle containing light rays associated with each focal points, as illustrated in Fig. 3. The ideal **EDoF** lens has the parameter l of which is infinite in length and the parameter w of which is infinitely thin. For the realistic **EDoF** lenses, however, the parameters l and w are typically on the order of microns.

The idea of **EDoF** lens as an optical element which focuses light into longitudinally directed line along the optical axis was first proposed by Golub, et. al. (**author?**) [8]. The idea was later adopted by others and it has found applications in various imaging systems, such as microscopes, cameras, and lithography to list a few, (**author?**) [2, 3, 4, 5, 9, 10, 11]. Alexander and Lukyanov have recently proposed a conceptual scheme for the **EDoF** lens(**author?**) [11]. Their scheme for **EDoF** lens consists of zones that are axially symmetric about the optical axis and this is illustrated in Fig. 4. The idea behind

their concept is as follows. The light ray crossing each zone gets focused to a unique spot on the optical axis and this spot is within in the **EDoF** lens parameter l . If β_i is the function which describes the focal length for the i th concentric zone in Fig. 4, the lens aperture, in principle, can be tailored to behave like **EDoF** lens by tweaking β_i . Borrowing their terminology, the β_i is referred to as the instantaneous focal function. The idea behind **EDoF** lens is to make l as large and w as small as possible. By experimenting with different functions for β_i , the **EDoF** lens parameters l and w can be engineered to the acceptable range for the imaging systems based on **SAIT** principle. This is exactly just what Alexander and Lukyanov did, and their focal function is summarized in Fig. 5. In the figure, the vertical lines represent discontinuities and each of the twelve zones has been indicated appropriately by a number. For each of the zones in Fig. 4, the incident parallel rays are focused at different points on the optical axis within l ; and, the focusing is described by the instantaneous focal function, $\beta = \beta_i$, summarized in Fig. 5.

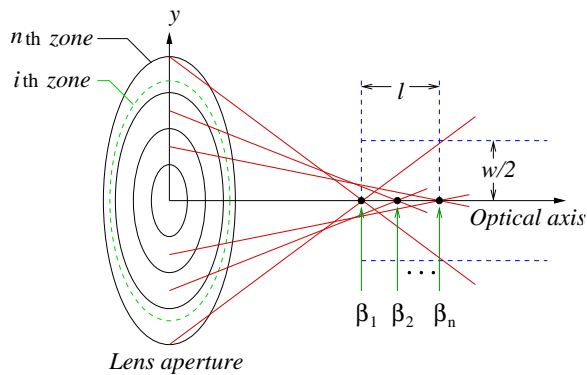


Figure 4: Schematic of conceptual **EDoF** lens proposed by Alexander and Lukyanov. The lens aperture has an axial symmetry about the optical axis.

The imaging system based on **SAIT** is a package solution in which both the hardware (optical element or **EDoF** lens) and the software (image reconstruction code base) contributions must be optimized. Alexander and Lukyanov experimented with various mathematical curves for the focal function β in an attempt to make the **EDoF** lens parameters l and w as ideal as possible, but did not attempt to provide any solutions concerning the physical shape or the profile for their conceptual **EDoF** lens. To test the image reconstruction code for the processing speed and the quality of generated image output, the information on the point spread function (or **PSF** for short) of the optical element input stage is required. Since no information on the physical profile of their conceptual **EDoF** lens was available, the test for their image reconstruction algorithm had to be deferred. It was my job to design a physical **EDoF** lens. Since Alexander's image reconstruction code was based on the

input from a lens aperture satisfying the focal function described in Fig. 5, the physical **EDoF** lens to be designed had a constraint of satisfying the same focal function characteristics. To end the story, the physical **EDoF** lens with such characteristics for the focusing behavior was found (author?) [12]. The obtained physical profile of lens was entered into CODE V®[17] to generate the needed **PSF** information for the lens aperture.[18] This information was in turn used by Alexander to test for the performance of his algorithm.

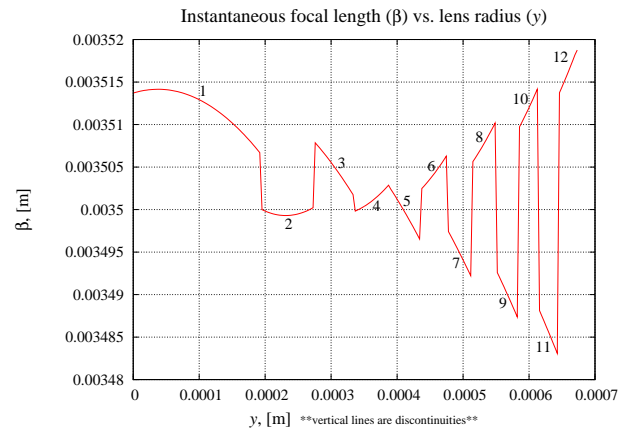


Figure 5: Focal function β proposed by Alexander and Lukyanov (author?) [11].

This work concerns the result of my role in the project, which was to design a physical **EDoF** lens from the focal function characteristics. As such, this work concerns the hardware contribution side of the optical imaging system based on **SAIT**.

II. THEORY

A. Axial symmetry

By definition, an axial symmetry is a symmetry about a given axis. The object has an axial symmetry if its appearance is unchanged with the rotation about some axis. Illustrated in Fig. 6 is a schematic of conceptual lens, which shows an axial symmetry about the optical axis, i.e., the x axis. Such a lens can be dissected through the origin with the xy plane as shown in Fig. 6. The curve traced on the xy plane, which is a set of points on the surface of lens, can be revolved about the optical axis for the three dimensional shape of the lens. The design of axially symmetric lens, therefore, simplifies to the problem of finding the set of points on the surface of lens of which gets traced on the xy plane.

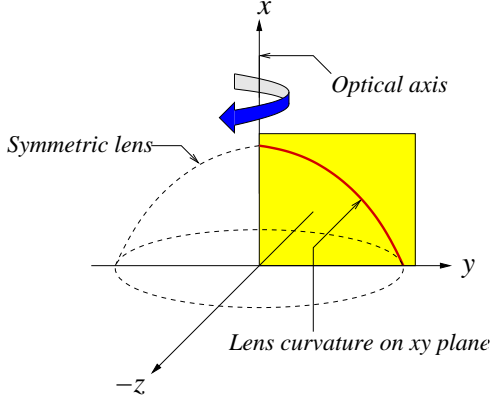


Figure 6: Schematic of lens symmetric about optical axis.

The physical law of which governs the bending of light is the Snell's law. I shall apply Snell's principle to derive the equation for the cross-sectional profile of the lens. The terminology, "cross-sectional profile of the lens," implies the lens curvature on the xy plane, which is illustrated in Fig. 6.

B. Derivation from Snell's law

When a ray of light passes across media of different refractive indices, its path is governed by the Snell's law,

$$n_\phi \sin \phi = n_\theta \sin \theta, \quad (1)$$

as illustrated in Fig. 7. Here, $n_\phi \equiv n_\phi(\omega)$ and $n_\theta \equiv n_\theta(\omega)$ are frequency dependent refractive indices with ω denoting the angular frequency of the light. The parameters ϕ and θ represent the angle of incidence and angle of refraction, respectively.

If \mathbf{N} denotes the normal vector to the local point $y = \gamma$ on the curve $x = h(y)$, then it can be shown

$$\|-\mathbf{N} \times (-\mathbf{e}_1)\| = \|-\mathbf{N}\| \|-\mathbf{e}_1\| \sin \phi = N \sin \phi$$

and the expression for $\sin \phi$ becomes

$$\sin \phi = \frac{\|\mathbf{N} \times \mathbf{e}_1\|}{N}, \quad N \equiv \|\mathbf{N}\|, \quad (2)$$

where \mathbf{e}_1 is the unit basis for the x axis.

Similarly, the expression for $\sin \theta$ may be obtained by considering vectors \mathbf{A} , \mathbf{B} , and \mathbf{C} of Fig. 7. The vectors \mathbf{A} , \mathbf{B} , and \mathbf{C} satisfy the relation,

$$\mathbf{A} + \mathbf{B} = \mathbf{C}. \quad (3)$$

In explicit form, vectors \mathbf{A} and \mathbf{B} are defined as

$$\mathbf{A} = -\gamma \mathbf{e}_2, \quad \mathbf{B} = (\beta - \alpha) \mathbf{e}_1, \quad (4)$$

where \mathbf{e}_2 is the unit basis for the y axis. With Eqs. (3) and (4), the vector \mathbf{C} becomes

$$\mathbf{C} = (\beta - \alpha) \mathbf{e}_1 - \gamma \mathbf{e}_2. \quad (5)$$

The vector cross product $\mathbf{N} \times \mathbf{C}$ is given by

$$\mathbf{N} \times \mathbf{C} = (\beta - \alpha) \mathbf{N} \times \mathbf{e}_1 - \gamma \mathbf{N} \times \mathbf{e}_2$$

and its magnitude becomes

$$\begin{aligned} \|\mathbf{N} \times \mathbf{C}\| &= \|(\beta - \alpha) \mathbf{N} \times \mathbf{e}_1 - \gamma \mathbf{N} \times \mathbf{e}_2\| \\ &= NC \sin \theta, \end{aligned} \quad (6)$$

where $N \equiv \|\mathbf{N}\|$ and $C \equiv \|\mathbf{C}\|$. Utilizing Eq. (5), C may be expressed as

$$C = (\mathbf{C} \cdot \mathbf{C})^{1/2} = [(\beta - \alpha)^2 + \gamma^2]^{1/2}$$

and the Eq. (6) is solved for $\sin \theta$ to yield

$$\sin \theta = \frac{\|(\beta - \alpha) \mathbf{N} \times \mathbf{e}_1 - \gamma \mathbf{N} \times \mathbf{e}_2\|}{N [(\beta - \alpha)^2 + \gamma^2]^{1/2}}. \quad (7)$$

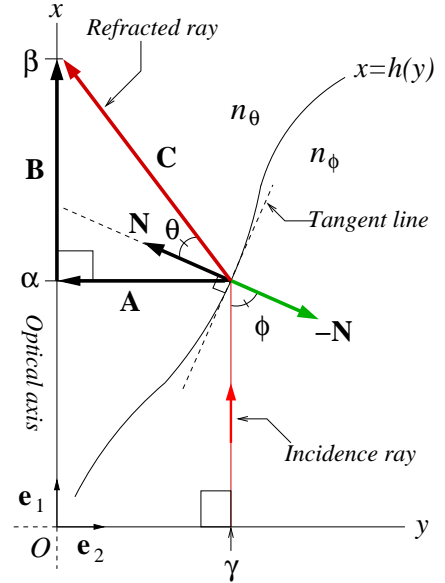


Figure 7: Illustration of Snell's law. The scalar quantity β denotes the focal length.

Insertion of Eqs. (2) and (7) into the Snell's law of Eq. (1) gives

$$\frac{n_\phi}{n_\theta} = \frac{\|(\beta - \alpha) \mathbf{N} \times \mathbf{e}_1 - \gamma \mathbf{N} \times \mathbf{e}_2\|}{\|\mathbf{N} \times \mathbf{e}_1\| [(\beta - \alpha)^2 + \gamma^2]^{1/2}}. \quad (8)$$

By definition, the normal vector \mathbf{N} satisfies the relation,

$$g(x, y) = x - h(y),$$

where $g(x, y)$ is a function whose gradient gives \mathbf{N} ,

$$\mathbf{N} = \nabla g = \frac{\partial g}{\partial x} \mathbf{e}_1 + \frac{\partial g}{\partial y} \mathbf{e}_2 = \mathbf{e}_1 - \frac{\partial h}{\partial y} \mathbf{e}_2.$$

Because \mathbf{N} is the normal vector at the location $(x = \alpha, y = \gamma)$, I write

$$\mathbf{N} = \mathbf{e}_1 - \frac{\partial h}{\partial y} \Big|_{y=\gamma} \mathbf{e}_2. \quad (9)$$

The following vector cross products are valid,

$$\begin{aligned} \mathbf{N} \times \mathbf{e}_1 &= \mathbf{e}_1 \times \mathbf{e}_1 - \frac{\partial h}{\partial y} \Big|_{y=\gamma} \mathbf{e}_2 \times \mathbf{e}_1, \\ \mathbf{N} \times \mathbf{e}_2 &= \mathbf{e}_1 \times \mathbf{e}_2 - \frac{\partial h}{\partial y} \Big|_{y=\gamma} \mathbf{e}_2 \times \mathbf{e}_2, \end{aligned}$$

where Eq. (9) was used to replace \mathbf{N} . Since $\mathbf{e}_1 \times \mathbf{e}_1 = \mathbf{e}_2 \times \mathbf{e}_2 = 0$, the previous relations reduce to

$$\mathbf{N} \times \mathbf{e}_1 = \frac{\partial h}{\partial y} \Big|_{y=\gamma} \mathbf{e}_3, \quad \mathbf{N} \times \mathbf{e}_2 = \mathbf{e}_3, \quad (10)$$

where \mathbf{e}_3 is the unit basis for the z axis of which satisfies the relation,

$$\mathbf{e}_1 \times \mathbf{e}_2 = \mathbf{e}_3, \quad \mathbf{e}_2 \times \mathbf{e}_1 = -\mathbf{e}_3.$$

Insertion of Eq. (10) into Eq. (8) gives

$$\frac{n_\phi}{n_\theta} = \frac{(\beta - \alpha) \frac{\partial h}{\partial y} \Big|_{y=\gamma} - \gamma}{\frac{\partial h}{\partial y} \Big|_{y=\gamma} [(\beta - \alpha)^2 + \gamma^2]^{1/2}},$$

which expression can be rearranged to yield

$$\frac{\partial h}{\partial y} \Big|_{y=\gamma} = \frac{\gamma}{\beta - \alpha - \frac{n_\phi}{n_\theta} [(\beta - \alpha)^2 + \gamma^2]^{1/2}}, \quad (11)$$

where α and γ are constants of which are depicted in Fig. 7.

For Alexander and Lukyanov's optical element, the instantaneous focal function $\beta \equiv \beta(y)$ in Eq. (11) is as defined in Fig. 5. The γ for the y axis is not anything special, of course. Any y belonging to the domain of h satisfies the Eq. (11). The generalization of Eq. (11) for all y belonging to the domain of h is done by making the following replacements:

$$\alpha \rightarrow x, \quad \gamma \rightarrow y, \quad \frac{\partial h}{\partial y} \Big|_{y=\gamma} \rightarrow \frac{\partial h}{\partial y} = \frac{dx}{dy}.$$

With these replacements, Eq. (11) gets re-expressed in form as

$$\frac{dx}{dy} = \frac{y}{\beta - x - \frac{n_\phi}{n_\theta} [(\beta - x)^2 + y^2]^{1/2}}. \quad (12)$$

How is the instantaneous focal function, β , restricted? The β in Eq. (12) is restricted so that the expression for

dx/dy does not blow up. Equation (12) is well defined if and only if the denominator satisfies the condition,

$$\beta - x - \frac{n_\phi}{n_\theta} [(\beta - x)^2 + y^2]^{1/2} \neq 0. \quad (13)$$

Contrarily, but equivalently, the previous statement can be reworded as follows. Equation (12) is ill defined if and only if the denominator satisfies the condition,

$$\beta - x - \frac{n_\phi}{n_\theta} [(\beta - x)^2 + y^2]^{1/2} = 0. \quad (14)$$

For reasons to follow, I shall proceed with the latter. To solve for β , I shall first rearrange Eq. (14) as

$$\beta - x = \frac{n_\phi}{n_\theta} [(\beta - x)^2 + y^2]^{1/2}. \quad (15)$$

Squaring of both sides give

$$(\beta - x)^2 = \frac{n_\phi^2}{n_\theta^2} (\beta - x)^2 + \frac{n_\phi^2}{n_\theta^2} y^2.$$

This expression can be rearranged to become

$$(\beta - x)^2 \left(1 - \frac{n_\phi^2}{n_\theta^2}\right) = \frac{n_\phi^2}{n_\theta^2} y^2$$

or

$$(\beta - x)^2 \left(\frac{n_\theta^2 - n_\phi^2}{n_\theta^2}\right) = \frac{n_\phi^2}{n_\theta^2} y^2.$$

And, solving for $(\beta - x)$, I obtain

$$\beta - x = \pm \frac{n_\phi y}{\sqrt{n_\theta^2 - n_\phi^2}}, \quad (16)$$

where the \pm came from the action of taking the square root on both sides, of course. Now, one of the signs in Eq. (16) can be eliminated by comparing with Eq. (15). This is the reason why I proceeded with Eq. (14) instead of Eq. (13). The n_ϕ and n_θ in Eq. (15) are both real refractive indices, which cannot be negative numbers. The instantaneous focal function, β , and the lens thickness, x , must be real, which implies $[(\beta - x)^2 + y^2]$ must be non-negative else $[(\beta - x)^2 + y^2]^{1/2}$ becomes an imaginary term. As real refractive indices cannot be negative numbers, the term $(\beta - x)$ is also a non-negative real in Eq. (15), provided $n_\phi > 0$, $n_\theta > 0$, and $[(\beta - x)^2 + y^2] > 0$, of course. Therefore, the right hand side of Eq. (16) must be positive; and, this gives

$$\beta = x + \frac{n_\phi y}{\sqrt{n_\theta^2 - n_\phi^2}}.$$

Now, this is precisely the condition for β which makes Eq. (12) ill defined. Equivalently, then Eq. (12) becomes well behaved for β satisfying the condition given by

$$\beta \neq x + \frac{n_\phi y}{\sqrt{n_\theta^2 - n_\phi^2}}. \quad (17)$$

Equation (17) defines the restriction for the instantaneous focal function, β .

What can be concluded of the restriction so defined in Eq. (17) for the instantaneous focal function? To answer this, recall that terms such as β , x , y , n_ϕ , and n_θ are all real values. And, there are no restrictions on n_ϕ and n_θ to speak of which of the two must be bigger or smaller in value. Interesting per se, the choice of $n_\phi > n_\theta$ results in the statement,

$$\beta \neq x + \frac{in_\phi y}{\sqrt{n_\phi^2 - n_\theta^2}}, \quad n_\phi > n_\theta, \quad (18)$$

where the i denotes the imaginary symbol and the term $\sqrt{n_\theta^2 - n_\phi^2}$ in Eq. (17) has been modified to $\sqrt{n_\phi^2 - n_\theta^2}$. But, this condition defined in Eq. (18) is always satisfied, as β is a real function. Therefore, it is concluded that Eq. (12) is well behaved everywhere for $n_\phi > n_\theta$.

III. RESULT

A. Lens surface equation

The profile of axially symmetric lens about its optical axis is obtained by solving the initial-value differential equation, Eq. (12),

$$\frac{dx}{dy} = \frac{y}{\beta - x - \frac{n_\phi}{n_\theta} \left[(\beta - x)^2 + y^2 \right]^{1/2}}, \quad x(y_0) = x_0,$$

where $x(y_0) = x_0$ is the initial condition to be specified and the instantaneous focal function β satisfies the constrain defined in Eq. (17). Without loss of generality, one may choose $x(y = y_0 = 0) = 0$ for the initial condition and the lens profile satisfies the differential equation,

$$\frac{dx}{dy} = \frac{y}{\beta - x - \frac{n_\phi}{n_\theta} \left[(\beta - x)^2 + y^2 \right]^{1/2}}, \quad (19)$$

$$x(0) = 0, \quad \beta \neq x + \frac{n_\phi y}{\sqrt{n_\theta^2 - n_\phi^2}}.$$

The quantities n_ϕ and n_θ are the two refractive indices in which one represents the lens and the other representing the surrounding medium. Which of the two refractive indices corresponds to the lens depends on the configuration of the problem, as demonstrated in the proceeding sections.

B. Alexander and Lukyanov lens

1. Instantaneous focal function

The instantaneous focal function proposed by Alexander and Lukyanov has been discussed previously in Fig. 5. The instantaneous focal function for each of the twelve zones can be curve fitted and represented by a quadratic polynomial of the form given by

$$\beta \equiv \beta_i = ay_i^2 + by_i + c, \quad y_{i,\min} \leq y_i \leq y_{i,\max}, \quad (20)$$

where the subscript i of $(\beta_i, y_i, y_{i,\min}, y_{i,\max})$ denotes the i th concentric zone. The coefficients a , b , and c , and the range for y , which defines the width for each of the axially symmetric concentric zones, are summarized in Table I. Since the instantaneous focal function, β , and the lens radius, y , have units of length measured in meters [m], the coefficient a must have a unit of $[\text{m}^{-1}]$, c a unit of [m], and b must be a unit-less scalar. To reduce the width of the table, couple columns were represented in millimeter units, [mm].

Table I: Domain y_i and coefficients (a, b, c) of $\beta_i = ay_i^2 + by_i + c$ for Fig. 5

$y_{i,\min}, y_{i,\max}$ [mm]	a [1/m]	b	c [mm]
0.0, 0.19182692	-313.07	0.0235	3.5137034
0.19519231, 0.27259615	534.53	-0.2472	3.527877626
0.27596154, 0.33317308	-309.02	0.0818	3.5088062
0.33653846, 0.38701923	536.05	-0.3275	3.5493232
0.39038462, 0.43413462	-306.12	0.1182	3.502912672
0.4375, 0.47451923	539.03	-0.3891	3.569538239
0.47788462, 0.51153846	-303.68	0.1463	3.496845208
0.51490385, 0.54855769	542.21	-0.4417	3.589312176
0.55192308, 0.58221154	-301.27	0.1695	3.49080193
0.58557692, 0.6125	545.96	-0.4895	3.609151039
0.61586538, 0.64278846	-298.81	0.1893	3.484870978
0.64615385, 0.67307692	179.08	-0.0474	3.469596542

2. Lens profile

Equation (19) was solved by the Runge-Kutta routine coded in **FORTRAN 90**(author?) [13]. For the computation, refractive indices, n_ϕ and n_θ , were chosen as follows,

$$n_\phi = 1.5311, \quad n_\theta = 1.0.$$

In this configuration, n_ϕ denotes the refractive index for the lens and n_θ denotes the refractive index for air.[19] The resulting cross-sectional profile of the lens curvature is shown in Fig. 8. The profile in Fig. 8 was revolved about the optical axis, which is the x axis in the figure, to generate the three dimensional profile of the physical

lens. This result is shown in Fig. 9, where the optical axis is located at $(\lambda y = 200, \lambda z = 200)$. The scaling factor of $\lambda = 3.365385 \times 10^{-6}$ was introduced for graphing purpose only.

In spite of the non constant β for the instantaneous focal function (see Fig. 5), the resulting **EDoF** lens shown in Figs. 8 and 9 seems to resemble the parabolic curve, which configuration is known to have only one focal point, i.e., $\beta = \text{constant}$. (author?) [14]. Is the result portrayed in Fig. 8 (or Fig. 9) correct? To give a qualitative answer to this, I shall recall the **EDoF** lens parameter l , which was previously illustrated in Fig. 3.

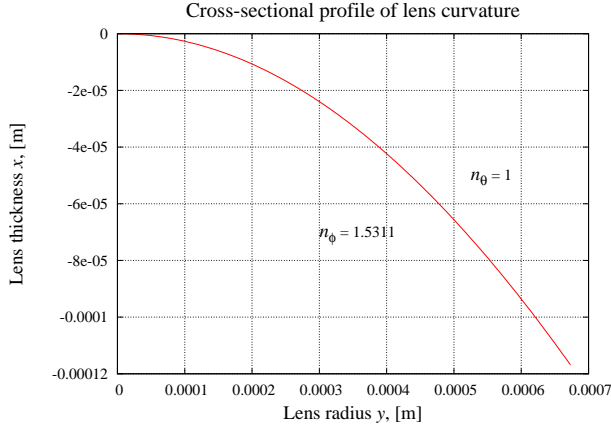


Figure 8: The cross-sectional profile of lens curvature corresponding to the instantaneous focal function proposed by Alexander and Lukyanov, Fig. 5.

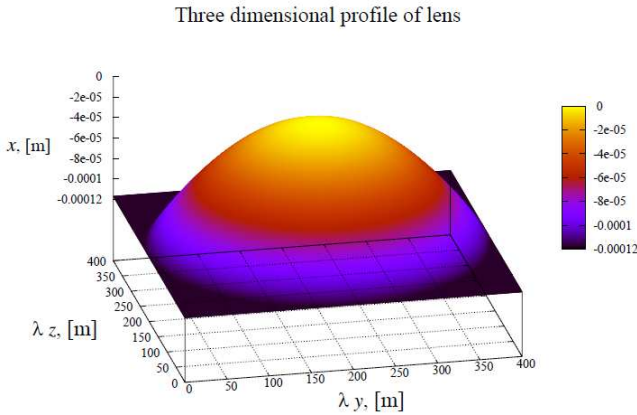


Figure 9: Three dimensional profile of lens satisfying the focal function β proposed by Alexander and Lukyanov, Fig. 5. The y and z axes have been multiplied by $\lambda = 3.365385 \times 10^{-6}$.

In explicit form, the **EDoF** lens parameter l is defined as

$$l = \|\beta_{\max} - \beta_{\min}\|, \quad \begin{cases} \beta_{\max} > 0, \\ \beta_{\min} > 0, \end{cases} \quad (21)$$

where β_{\max} and β_{\min} denote, respectively, the maximum and the minimum values in the profile of instantaneous focal function. In the focal function profile of Alexander and Lukyanov, Fig. 5, $\beta_{\max} \approx 3.5188$ mm and $\beta_{\min} \approx 3.4831$ mm. Plugging the information into Eq. (21), this roughly gives $l \approx 36$ μm . The resemblance of the **EDoF** lens to the parabolic curve can be attributed to the small value for l . Considering that Alexander and Lukyanov's lens has a maximum radius of $y \approx 0.67$ mm, which can be identified from Table I, the lens diameter comes out to be about $d = 2y \approx 1.34$ mm. This implies, the lens diameter is larger than the **EDoF** lens parameter, l , by a factor of thirty seven. Under such circumstance, the lens could be perceived as having a single focal point from the perspective of human eye. In spite of the existence of number of very closely spaced focal points within the length of l along the optical axis, the human eyes do not have sufficient resolving power to distinguish those focal points. Even less so, the human eyes cannot distinguish the actual cross-sectional profile of the lens of which is only slightly perturbed from the cross-sectional profile of the parabolic lens. To prove that this is indeed the case, I shall use the derived lens formula, Eq. (19), to generate various parabolic lenses.

C. Validation of the result

How does one know that Eq. (19) generates the correct profile for the lens? The easiest way to settle this dilemma is to actually apply Eq. (19) to the well known types, i.e., the parabolic lenses.

1. Simple parabolic lens

The parabolic curves are known to merge parallel rays of incidence light to a unique focal point called a focus (author?) [14]. As a consequence of this, the parabolic curves flatten in the curvature with the focus positioned at distances further from the vertex. Such property of parabolic curves make them ideal for testing and validating the lens formula defined in Eq. (19). The constant focus of $\beta = 1$ m, $\beta = 5$ m, and $\beta = 10$ m were considered to generate curves using Eq. (19); and, the result is summarized in Fig. 10. As expected, the generated curves are that of parabolic curves in which each curves corresponds to focal points $\beta = 1$ m, $\beta = 5$ m, and $\beta = 10$ m. The curve corresponding to $\beta = 10$ m is more flat in curvature than the ones corresponding to $\beta = 1$ m or $\beta = 5$ m, as expected. The result corresponding to $\beta = 1$ m was revolved about the optical axis to illustrate the three dimensional profile of the parabolic lens. This is shown in Fig. 11. Again, in the figure, the optical axis is at $(\lambda y = 200, \lambda z = 200)$, where the scaling factor λ is $\lambda = 3.365385 \times 10^{-6}$.

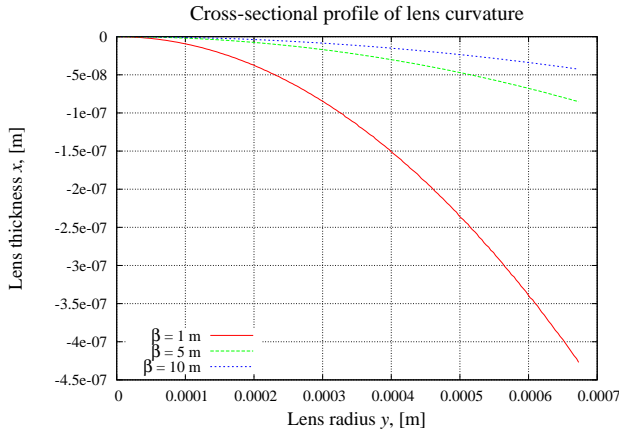


Figure 10: The cross-sectional profile of lens curvature for $\beta = 1$ m, $\beta = 5$ m, and $\beta = 10$ m.

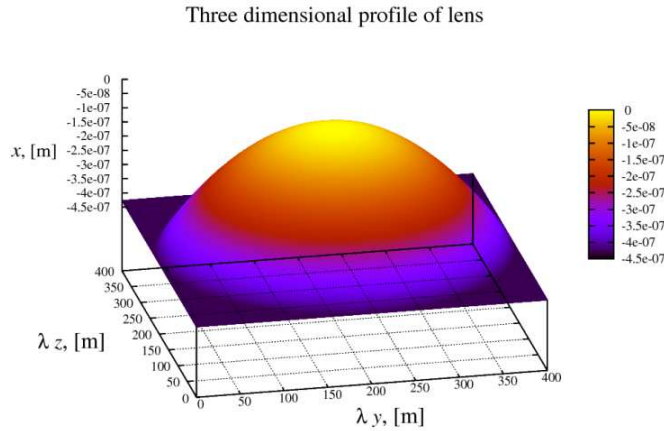


Figure 11: Three dimensional profile of a lens with a constant instantaneous focal function, $\beta = 1$ m. The y and z axes have been multiplied by $\lambda = 3.365385 \times 10^{-6}$.

2. Concentric parabolic lens

Now I consider a slightly more complicated profile for the instantaneous focal function, β . To show that, indeed, the likeliness of Alexander and Lukyanov's **EDoF** lens to the parabolic lens is attributed to the small value for the **EDoF** lens parameter l , I shall modify only the β portion of Alexander and Lukyanov's profile for the instantaneous focal function, while leaving the size of lens diameter unmodified. The modified focal function for this test is shown in Fig. 12. And, the coefficients a , b , and c , and the range of y corresponding to the $\beta \equiv \beta_i$ of Eq. (20) for each of the twelve zones is summarized in Table II. Besides the increased focal length for each of twelve zones, the focal point is unique within each zones in this test configuration. In Alexander and Lukyanov's focal profile, l was much smaller than the lens diameter d , i.e., $d \approx 37l$. The β_{\max} and β_{\min} for the test configura-

tion are, respectively, $\beta_{\max} = 2.5$ m and $\beta_{\min} = 0.01$ m, which can be verified from Table II. Using the formula for l defined in Eq. (21), this gives $l \approx 2.49$ m. Therefore, in this test configuration, l is much larger than d , i.e., $d \approx 5.4 \times 10^{-4}l$, which is just the opposite situation from that of Alexander and Lukyanov. That being said, the Eq. (19) was plotted for the curve and the result is shown in Fig. 13. As expected, the resulting cross-sectional profile for the lens does not resemble simple parabolic lens. However, the curve profile for each of the twelve zones in Fig. 13 represents the portion of a parabolic curve corresponding to β_i illustrated in Fig. 12. By superimposing the two graphs, Figs. 12 and 13, the boundaries for each zones can be identified by kinks in Fig. 13. The cross-sectional profile of the lens curvature illustrated in Fig. 13 was revolved about the optical axis for the three dimensional profile of the lens. This result is shown in Fig. 14.

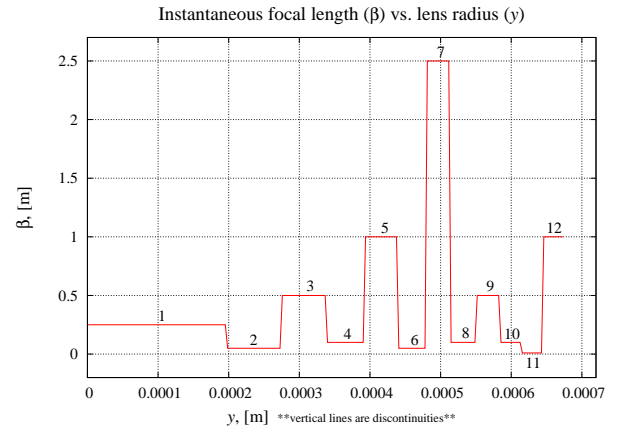


Figure 12: Focal function β with characteristic of a step function.

Table II: Domain y_i and coefficients (a, b, c) of $\beta_i = ay_i^2 + by_i + c$ for Fig. 12

$y_{i,\min}, y_{i,\max}$ [mm]	a [1/m]	b	c [m]
0.0, 0.19182692	0.0	0.0	0.25
0.19519231, 0.27259615	0.0	0.0	0.05
0.27596154, 0.33317308	0.0	0.0	0.50
0.33653846, 0.38701923	0.0	0.0	0.10
0.39038462, 0.43413462	0.0	0.0	1.00
0.4375, 0.47451923	0.0	0.0	0.05
0.47788462, 0.51153846	0.0	0.0	2.50
0.51490385, 0.54855769	0.0	0.0	0.10
0.55192308, 0.58221154	0.0	0.0	0.50
0.58557692, 0.6125	0.0	0.0	0.10
0.61586538, 0.64278846	0.0	0.0	0.01
0.64615385, 0.67307692	0.0	0.0	1.00

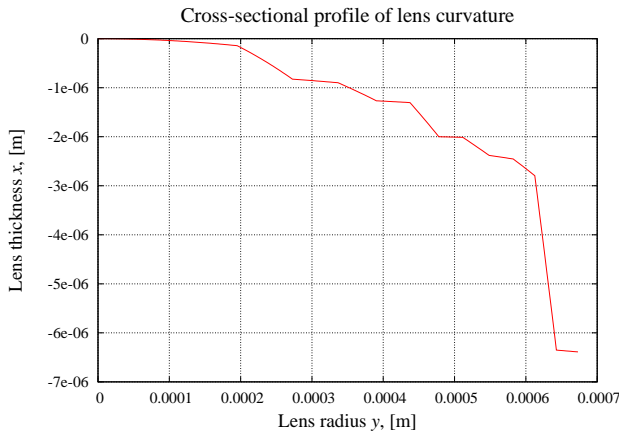


Figure 13: The cross-sectional profile of lens curvature corresponding to the focal function defined in Fig. 12.

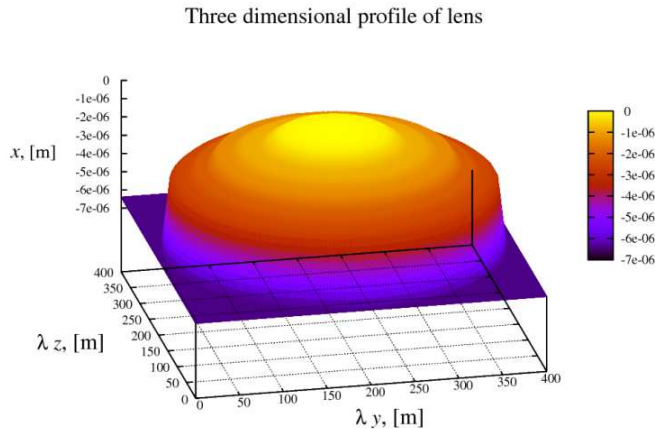


Figure 14: Three dimensional profile of lens satisfying the focal function defined in Fig. 12. The y and z axes have been multiplied by $\lambda = 3.365385 \times 10^{-6}$.

Basing on these results, it can be concluded that for the case where the lens diameter d is much larger than the **EDoF** lens parameter l , the profile of the lens re-

sembles closely the profile of simple parabolic lens. Here, the word “simple” has been used to denote the parabolic curve with single focus. In the opposite situation, where the lens diameter d is much smaller than the **EDoF** lens parameter l , the profile of the lens no longer resembles the simple parabolic lens. Instead, in this latter case, the shape for the lens resembles superimposed, multiple number of parabolic lenses of different degrees of curvature, as illustrated in Fig. 14.

IV. CONCLUDING REMARKS

The image processing speed and the quality of processed images are both of critical importance in software assisted imaging technology. Such a requirement calls for the optimization of image reconstruction code based on the principles of wave optics. The coding side of the **SAIT** system can be optimized if **EDoF** lens is used for the input stage.

In this presentation, the formula for the **EDoF** lens has been derived based on the knowledge of instantaneous focal function, β . The β information is an important tool in the design of **EDoF** lens, as this allows optical engineer to try out various mathematical curves using computers for optimization. With the knowledge of β , this can be achieved without having to actually make **EDoF** lens prototypes, thereby saving time and the cost. Once the optimal solution for the instantaneous focal function is obtained, the physical **EDoF** lens can be manufactured based on the lens formula presented in this work.

V. ACKNOWLEDGMENTS

I would like to thank G. Alexander for providing the raw data for the focal function. I would also like to thank Dr. S. Lee for generating the **PSF** information for the lens designed in this work using **CODE V**®. The author acknowledges the support for this work provided by Samsung Electronics, Ltd.

-
- [1] Wikipedia, “Depth of Field,” http://en.wikipedia.org/wiki/Depth_of_field.
 - [2] V. Portney, “Multifocal Ophthalmic Lens,” U.S. Patent 4898461 (1990).
 - [3] D. Mendlovic, Z. Zalevsky, G. Shabtay, U. Levy, E. Marom, and N. Konforti, “Synthesis of light beams,” U.S. Patent (2002).
 - [4] E. Ben-Eliezer, Z. Zalevsky, E. Maron, N. Konforti, and D. Mendlovic, “All optical extended ‘depth-of-field’ imaging system,” U.S. Patent 7158317 (2007).
 - [5] E. Dowski, “Wavefront coding optics,” U.S. Patent 6842297 (2005).
 - [6] S. Bradburn, W. Cathey, E. Dowski, “Realization of focus invariance in optical-digital systems with wave-front coding,” *Appl. Opt.* **36**(35), pp. 9157-9166 (1997).
 - [7] E. Dowski, Jr., and W. Cathey, “Extended depth of field through wave-front coding,” *Appl. Opt.* **34** (11), pp. 1859-1866 (1995).
 - [8] M. Golub, D. Leonid, N. Kazanskiy, S. Kharitonov, I. Sisakian, and V. Soifer, “Focusators at letters diffraction design,” in *Proceedings of SPIE*, Vol. **1500**, 211 (1991).
 - [9] B. Forster, D. Van De Ville, J. Berent, D. Sage, and M. Unser, “Extended Depth-of-Focus for Multi-Channel Microscopy Images: A Complex Wavelet Approach,” in *Proceedings of the Second IEEE International Symposium on Biomedical Imaging: From Nano to Macro (ISBI’04)*, (Arlington VA, USA, April 15-18, 2004), pp. 660-663.
 - [10] Z. Liu, A. Flores, M. Wang, and J. Yang, “Diffractive

- infrared lens with extended depth of focus,” *Optical Engineering* **46**(1), 018002 (2007).
- [11] G. Alexander and A. Lukyanov, “Lens with extended depth of focus and optical system having the same,” Korean Patent 10-2008-0043428 (2008), <http://www.kipo.go.kr>.
- [12] S. Cho, “Method for designing physical lens from depth of focus characteristics and lens with extended depth of focus designed by the same method,” Korean Patent 10-2008-0111002 (2008), <http://www.kipo.go.kr>.
- [13] W. Derrick and S. Grossman, *A First Course in Differential Equations with Applications* (West Publishing Company, St. Paul, 1987).
- [14] G. Thomas and R. Finney, *Calculus and analytic geometry*, 7th Ed, (Addison-Wesley, USA, 1988).
- [15] According to the industry standard of specifications set by the flat panel display consortium, the **1080P** specification of the full-**HD** quality of liquid crystal displays (**LCDs**) process sixty image frames per second.
- [16] Unfortunately, the work place I am affiliated with, Samsung Advanced Institute of Technology, also uses the abbreviation “SAIT” for the name. To distinguish this SAIT from software assisted imaging technology, I denote the latter with bold faced version, **SAIT**.
- [17] CODE V[®] is an optical design program with graphical user interface for image forming and fiber optical systems by Optical Research Associates (ORA), an organization that has been supporting customer success for over 40 years, www.opticalres.com.
- [18] Using CODE V[®] to obtain **PSF** information turned out to be a nontrivial task, as the built-in curve fitting functions for CODE V[®] were not too “happy” with the obtained result for the surface profile of **EDoF** lens.
- [19] Although the actual value varies depending on the surrounding humidity and so on, the refractive index of an air is about $n \approx 1.0008$.